

See discussions, stats, and author profiles for this publication at: <https://www.researchgate.net/publication/311452634>

Aluminum Nitride Nanotubes

Article in *Chemical Papers* · December 2016

DOI: 10.1007/s11696-016-0015-5

CITATIONS

0

READS

125

3 authors:



[Maziar Noei](#)

Islamic Azad University

59 PUBLICATIONS 306 CITATIONS

[SEE PROFILE](#)



[Hamed Soleymanabadi](#)

Islamic Azad University

34 PUBLICATIONS 233 CITATIONS

[SEE PROFILE](#)



[Ali Ahmadi Peyghan](#)

Tarbiat Modares University

163 PUBLICATIONS 2,756 CITATIONS

[SEE PROFILE](#)

Some of the authors of this publication are also working on these related projects:



explosive nanomaterials [View project](#)



DFT calculations on Nano materials [View project](#)

All content following this page was uploaded by [Ali Ahmadi Peyghan](#) on 06 December 2016.

The user has requested enhancement of the downloaded file. All in-text references [underlined in blue](#) are added to the original document and are linked to publications on ResearchGate, letting you access and read them immediately.



Aluminum nitride nanotubes

Maziar Noei¹ · Hamed Soleymanabadi² · Ali Ahmadi Peyghan³

Received: 2 August 2016 / Accepted: 14 October 2016

© Institute of Chemistry, Slovak Academy of Sciences 2016

Abstract An AlN nanotube (AlNNT) was theoretically predicted in 2003. In comparison with the carbon nanotubes, the AlNNTs are wide-band-gap nanostructures with high reactivity, high thermal stability and sharp electronic sensitivity toward some chemicals. The B3LYP predicts an HOMO–LUMO gap of 3.74–4.27 eV for *zigzag* AlNNTs, while the experimental band gap of bulk AlN is about 6.28 eV. The lowest strain energy of AlNNTs relative to its AlN nanosheet compared to the nanosheets of carbon and BN nanotubes with an equivalent diameter suggests the feasibility of AlNNT synthesis from its nanosheet. Theoretical methods predict a Young's Modulus of about 453 GPa for AlNNTs that is smaller than that of carbon (1 TPa), BN (870 GPa) and GaN (796 GPa) nanotubes. In 2003, the faceted single-crystalline hexagonal AlNNTs were synthesized and extensively explored by means of density functional theory calculations. Several works have suggested different potential applications for AlNNTs including chemical sensors, hydrogen storage, gas adsorbent, and electron field emitter. This review is a comprehensive study on the latest achievements in the structural analyses, synthesis, and property evaluations based on the computational methods on the AlNNTs in the light of the development of nanotubes.

Keywords Nanostructures based on AlN · Aluminum nitride nanotube · Computational study · Wide-band-gap systems · Sensor

Introduction

From the time when carbon nanotubes (CNTs) have been discovered (Iijima 1991) and their extensive possible applications (Beheshtian et al. 2012a, b, c, d, e, f, g, h, i, j; Parlayici et al. 2015; Baei et al. 2012a, b, c; Robati et al. 2016; Shamsudin et al. 2013; Sreekala et al. 2013; Saha and Das 2014; Goodarzi et al. 2015), intensive attentions have been devoted to non-carbon nanotubes (Beheshtian and Peyghan 2013; Peyghan and Bagheri 2012; Baei et al. 2012a, b, c, 2013; Beheshtian et al. 2013a, b, c, d, e; Peyghan et al. 2012a, b). Examples are the nanotubes of $B_xC_yN_z$ composites, metal oxides such as MgO, ZnO and WS_2 , the halogen compound of NiC_{12} , silica and polyaniline nanotubes (Altoe et al. 2003; Stejskal et al. 2009; Kim et al. 2011; Hacoheh et al. 1998; Cui et al. 2012). Among these compounds, group III nitride nanostructured materials are mostly fascinating because the wurtzite nitrides yield a continuous alloy structure with variable band gaps from 1.9 to 6.2 eV (Beheshtian et al. 2012a, b, c, d, e, f, g, h, i, j, 2013a, b, c, d, e; Peyghan et al. 2013a, b, c). The AlN is a wide-band-gap material, exhibiting high hardness, high stability, high thermal conductivity, and low coefficient of thermal expansion, and it is frequently used in thin film devices as a substrate (Yim et al. 1973). During the last decade, numerous efforts have been dedicated to synthesis, characterization, and potential applications of AlN nanotubes (AlNNTs) (Balasubramanian et al. 2004; Yin et al. 2005). The most promising applications include chemical sensors, hydrogen storage, and field emitters (Baei et al.

✉ Ali Ahmadi Peyghan
ahmadi.iau@gmail.com

¹ Department of Chemistry, Mahshahr Branch, Islamic Azad University, Mahshahr, Iran

² Young Researchers and Elite Club, Yadegar-e-Imam Khomeini (RAH) Shahr-e-Rey Branch, Islamic Azad University, Tehran, Iran

³ Young Researchers and Elite Club, Islamshahr Branch, Islamic Azad University, Islamshahr, Iran

2012a, b, c; Noei et al. 2015; Shi et al. 2005; Wang et al. 2009; Ahmadi et al. 2012). This contribution provides a comprehensive review on the AlNNT field, and systematically summarizes respected successes in synthesis, morphology, potential applications and predictions on the various properties.

Theoretical prediction

Zhang and Zhang (2003) have theoretically explored the possibility of synthesis and different properties of AlNNTs using different models (Fig. 1). The nanotube structure which was studied in their work was single-walled with an *armchair* chirality, and the geometries were relaxed at the Hartree–Fock (HF) level of theory with 3-21G* basis set. They deduced that AlNNTs are thermodynamically favorable with a uniform diameter and smooth tubular surface, in comparison to the experimentally observed CNTs and AlN nanowires. Aluminum and nitrogen atoms arrange in a hexagonal network in the tube wall, adopting an sp^2 hybridization. The calculated eigenvalues of HOMO and LUMO were about -0.34226 (-9.31 eV) and 0.05823 a. u. (1.58 eV); thus, the HOMO–LUMO gap is 10.89 eV. It should be noted that what they have calculated is HOMO–LUMO gap, not band gap, as mentioned in the original paper (Zhang and Zhang 2003). Band gap in the solid-state physics refers to the difference in energy between the bottom of the conduction band and the top of the valence band, corresponding to the energy difference between the electron affinity and ionization potential of the material (Cui et al. 2012).

The unusually large HOMO–LUMO gap is originated from the disadvantage of HF theory in predicting the HOMO, and LUMO levels, and also the size influence of nanotubes (Zhang et al. 1996). In the HF model, the LUMO sees one electron more (N instead of $N - 1$) than the HOMO; therefore, the LUMO is shifted to much higher energy, overestimating the HOMO–LUMO gap. The model nanotubes were finite-sized and their ends were saturated with H atoms to decrease the boundary effect (Bredas 2014). It should be noted that the real nanotubes are much longer and did not have any hydrogen atoms. A nanotube with a greater diameter and length is expected to have lower strain energy and, therefore, higher stability. Finally, it has been suggested that the synthesis of AlNNTs may be a potential achievement in future (Bredas 2014).

However, unlike BN nanotubes (BNNTs) which possess honeycomb graphitic framework on the single walls of the tube (Golberg et al. 1996), so far, no experimental synthesis of analogous geometries in AlNNTs has been reported. Undoubtedly, this difference is because of the existence of BN graphene-like nanosheets which can be

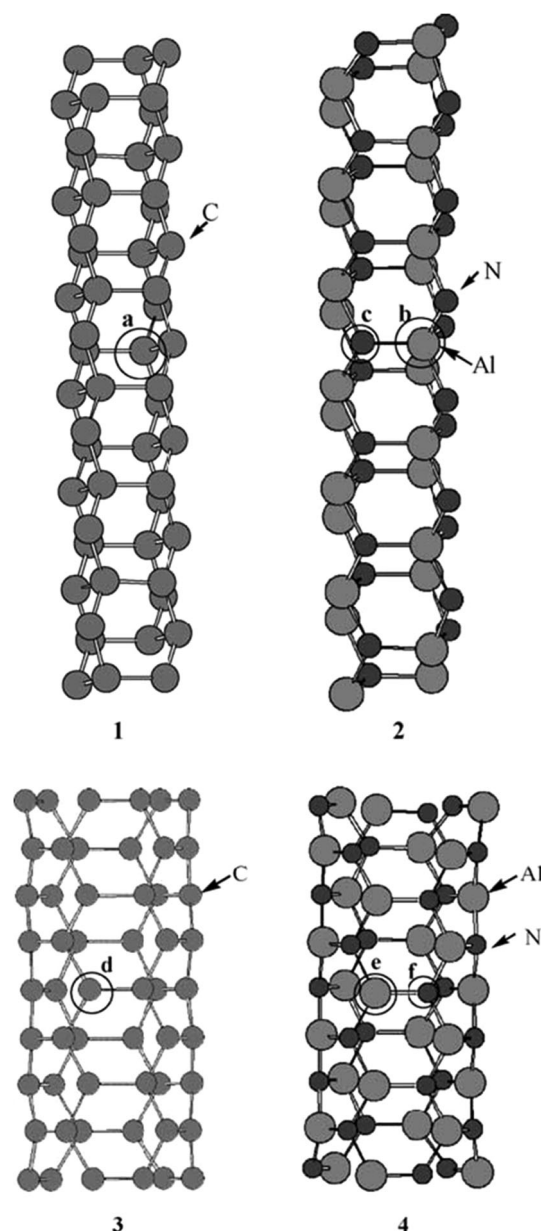
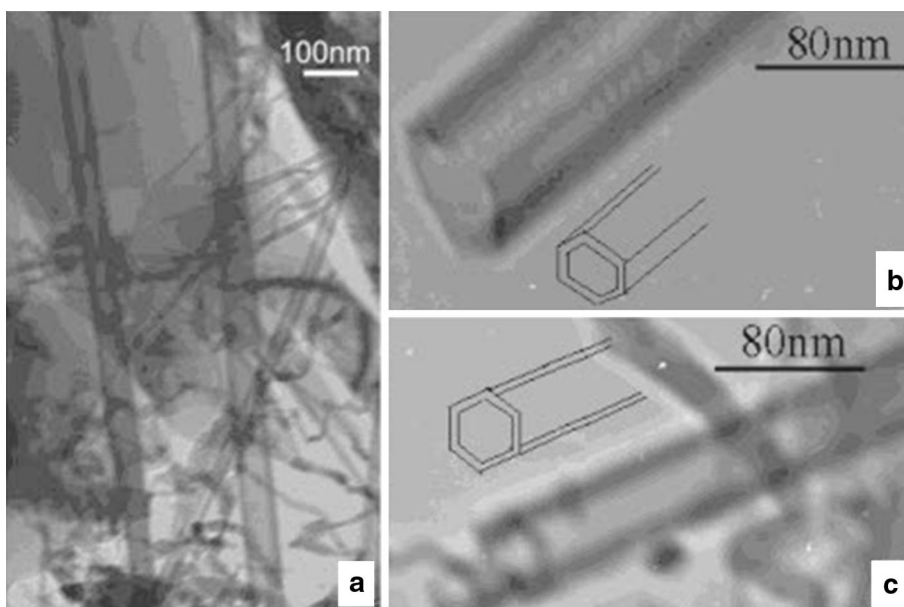


Fig. 1 Models demonstrating the various models used in (Stejskal et al. 2009), where the *circled atoms* are chosen as the representative atoms of each of the model systems: a diamond nanowire $c\text{-C}_{54}$ (1), an AlN nanowire $c\text{-Al}_{27}\text{N}_{27}$ (2), a carbon nanotube $h\text{-C}_{54}$ nanotube (3) and AlN nanotube $h\text{-nitride AlN}$ nanotube $h\text{-Al}_{27}\text{N}_{27}$ (4)

rolled up in BN nanotubes, while AlN nanosheets are rather metastable or unstable. The stability of an infinite hexagonal AlN ($h\text{-AlN}$) sheet and its structural and electronic properties have been studied within the framework of DFT at the GGA-PBE level of theory, demonstrating, qualitatively, synthesizability of individual $h\text{-AlN}$ sheets (Almeida et al. 2012). Although, graphite-like $h\text{-AlN}$ multilayers have been experimentally observed and theoretically modeled (Santos et al. 2016), the synthesis of monolayer graphene-like $h\text{-AlN}$ has not been reported yet.

Fig. 2 **a** TEM image of the AlN product containing nanotubes and nanowires. **b**, **c** Pseudo-hexagonal open ends of two AlN nanotubes in different lying fashions as schematically shown in the figures. For faceted tubular structure, different lying fashions will result in different numbers of distinguishable contrast regions as seen here



Synthesis

Wu et al. (2003) synthesized the faceted single-crystalline hexagonal AlNNTs by nitriding the Al powder, impregnating with CoSO_4 (1.0 mmol Co per gram of Al) in advance, with NH_3/N_2 (NH_3 4 vol%). The transmission electron microscopic (TEM) images (Fig. 2) show that the product is a blend of nanowires and nanotubes. Most AlNNTs have both ends open and their lengths are few micrometers and the diameters are in the range of 30–80 nm. It has been detected that the ends of the tubes have the pseudo-hexagonal shape (Fig. 2). However, the results provided an alternative AlNNT with N and Al atoms [compared to the theoretical results of (Bredas 2014)] still positioning in hexagonal crystalline arrangement, analogous to the case for bulk h-AlN, and a non-layered construction is detected. In this construction, each atom has one dangling bond; thus, surface passivation is commonly unavoidable.

Balasubramanian et al. (2004) have synthesized the AlNNTs using solid–vapor equilibrium by gas-phase condensation. The tubes were dispersed on an extremely oriented pyrolytic graphite sheet. The scanning tunneling microscopy measurements have been performed in a vacuum chamber at room temperature by an OMICRON STM/AFM system. Diverse structures including nanotubes and nanoparticles have been observed (Fig. 3). The AlNNTs are a mixture of a single tube and also tubes as groups of three or four ones as wide as a few micrometers. They are mostly in helicoidal or twisted arrangement with diameter of about 0.8–3.0 nm. It has been predicted that the AlNNT construction consists of, chiefly, hexagons of N and Al atoms which adopt sp^2 hybridization, thereby confirming

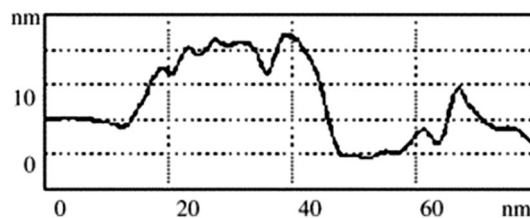
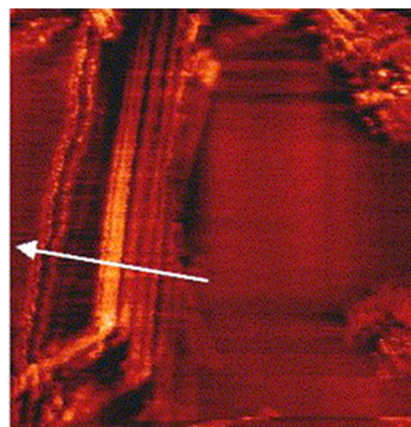


Fig. 3 STM image (160×160 nm) showing bundles of twisted AlN nanotubes and nanoparticles. The flat surface is highly oriented pyrolytic graphite. A line profile is also reported to show the height of the nanotubes. The white line is only a guideline for the eye to follow the curling direction of the tube along its axis (white arrow)

the computational predictions (Bredas 2014). This explanation is deep-rooted by comparing the computed interatomic distance (0.32 nm) and the average distance between two N (0.306 nm), or two Al atoms with the results of Ref. (Bredas 2014).

Yin et al. (2005) have reported the first synthesis of coaxial C–AlN–C combined nanotubes created in bulk

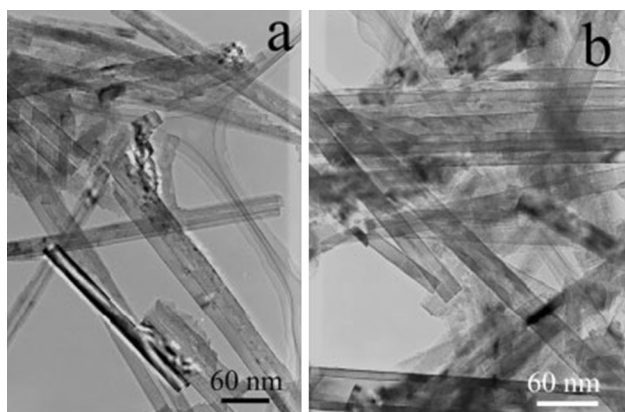
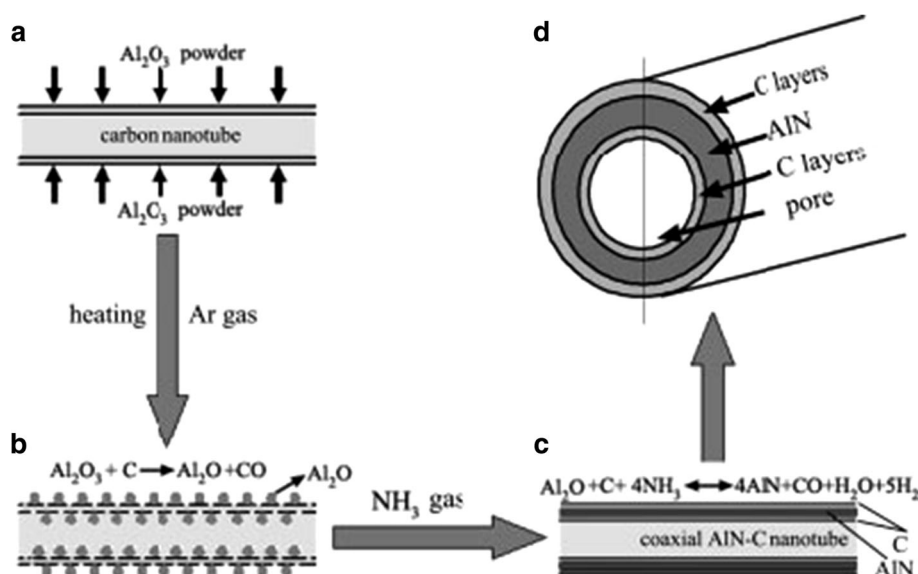


Fig. 4 a, b Low-magnification TEM images of the synthesized AlN nanotubes

quantities through a reaction of chemical substitution in a manageable two-step process using CNTs as templates. They showed that the C–AlN–C nanotubes are slightly faceted because of a confinement effect of the CNT templates. Therefore, only faceted single-crystalline AlNNTs with a non-layered structure were finally formed. The length of the AlNNTs was about several micrometers, and the outer diameter was approximately between 45 and 50 nm, with walls of 13-nm thickness. The synthesized AlNNTs were straight (in contract to the results of Ref. (Wu 2009)) and the TEM images (Fig. 4) show that most of them are open-ended. Chemically, the coaxial C–AlN–C nanotube formation is a carbonitridation route, in which CNTs act as reducing material and templates for the AlNNT creation. The coaxial C–AlN–C composite nanotube formation is shown in Fig. 5.

Fig. 5 Schematic illustration of the formation process of C–AlN–C composite nanotubes. **a** Al₂O₃ powders are coated on the surface of carbon nanotubes. **b** Al₂O₃ adsorbed on the surface of MWCNTs reacts with them to form Al₂O through a chemical reaction. **c** Under a continuous NH₃ flow, Al₂O reacts with NH₃ and C to form AlN nanotubes through a chemical reaction. The carbon layers form on both the outer and inner surfaces of AlN tubes during the reverse reaction. **d** Cross-el of C–AlN–C composite nanotubes



Stability and strain energy

The p orbital character of HOMO of an AlNNT like that of CNT predicts the probability of AlNNT formation (Bredas 2014). The strain energies needed to generate nanotubes from their graphene-like nanosheets, and their thermal stability are main factors in anticipating the formation of tubular geometries (Tenne and Zettl 1996). In a theoretical work, Zhao et al. (2003) have assessed the strain energy needed to roll up an AlN nanosheet into an AlNNT using DFT calculations, comparing it with the results of carbon, GaN, and BN nanotubes. They used ab initio code of SIESTA with the exchange–correlation functional of Perdew, Burke and Ernzerhof and the basis set of double- ζ plus polarization orbitals (Zhao et al. 2003). They employed periodical boundary condition along the AlNNT axis. The average Al–N bond length has been computed to be 1.83 Å which is slightly smaller than that of the cubic AlN which is about 1.89 Å (Pentaleri et al. 1997).

It was found that the buckling in AlNNTs is smaller, compared to that of GaN and BN nanotubes with comparable diameters. To evaluate the thermal stability, they modeled the annealing route of an (5,5) *armchair* AlNNT for 2 ps at 1000 K, using first-principles molecular dynamics (Zhao et al. 2003). The tubular construction was maintained even at high temperature, and the tube wall buckling was very small so that the structural deformation can be recovered by re-optimization. They suggested this phenomenon as a reason for the high thermal stability of AlNNTs.

Figure 6 (Zhao et al. 2003) shows the computed strain energy per atom needed to roll up an AlN nanosheet into an

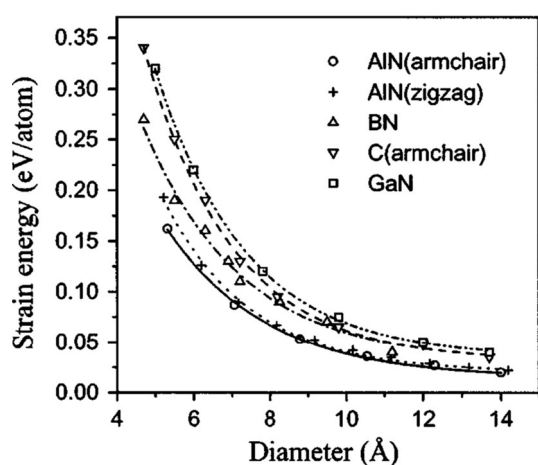


Fig. 6 Strain energy vs diameter for the formation of AlN *armchair* and *zigzag* nanotubes relative to their sheet structures. The strain energies of BN, GaN, and carbon nanotubes are also presented for comparison. The curves are fitted by the least-square method

AlNNT of a specified diameter. For comparison, the energy costs for the formation of carbon, BN, and GaN nanotubes are also given in Fig. 6. As it can be seen, by increasing the diameter of the tubes, the strain energy decreases. Also, the strain energies are independent of chirality, in the case of BN (Pentaleri et al. 1997) and GaN (23 Lee et al. 1999) nanotubes. This is in good contrast with the results of (Oh and Lee 1998) which indicate that *armchair* CNTs are more stable than *zigzag* ones. The lowest strain energy of AlNNTs relative to its nanosheet in comparison to those of BN and CNTs with a comparable diameter proposes the feasibility of AlNNT synthesis from a graphene-like AlN. Stan et al. (2008) have reported the synthesis of faceted AlNNTs through an ‘epitaxial casting’ process like that reported for the GaN nanotube synthesis (Goldberger et al. 2003). First, they used triangular faceted GaN nanowires synthesized by Ni-catalyzed metal–organic chemical vapor deposition (MOCVD) at 800 °C, and then, AlN shells were grown around the GaN nanowires by MOCVD at 1000 °C. Subsequently, the GaN cores were removed by annealing at 1120 °C in hydrogen atmosphere, leaving behind the empty AlN shells.

The MOCVD method is a highly complex procedure for growing crystalline layers, employed in the manufacturing of transistors, light-emitting diodes (LEDs), solar cells, lasers, and different electronic devices (Nishizawa and Kurabayashi 1983; Liu et al. 2000; Kakanakova-Georgieva et al. 2006; Choi et al. 2012). Also, sublimation epitaxy of AlN has been performed on 4H-SiC (Kakanakova-Georgieva et al. 2004), resulting in AlN pattern consisting of individual single wurtzite AlN crystallites with plate-like shape aligned along [1 $\bar{1}$ 0 0] direction. In contrast to epitaxy method, the growth of crystals in MOCVD is by chemical reaction and not physical deposition. The

MOCVD method is more favorable for formation of devices that are thermodynamically metastable.

Mechanical properties

“A reaction to an applied load” may be a proper definition for mechanical properties of materials. These properties may delineate the range of utility of a substance and establish the service life can be anticipated. There exist a few studies on the mechanical properties of AlNNTs of which most of them are theoretical studies.

Young’s moduli

The Y indicates the ratio of stress (force per unit area) and strain (proportional deformation) in a material and is a measure of the stiffness. The typical equation for Young’s modulus is:

$$Y = (F/a)/(\Delta l/l_0) , \quad (1)$$

where a is the cross-sectional area and l_0 is the nanotube length. Kang and Hwang (2004) have calculated the Young’s moduli of single-wall (5,5) *armchair* AlNNTs, BN and GaN nanotubes (BNNTs and GaNNTs) using simulations. Their calculations showed that the Young’s modulus of AlNNTs is about 453 GPa. An experimental work has reported this value to be about 250–400 GPa for faceted AlNNTs (Stan et al. 2008). This is smaller than Young’s moduli of CNT which is about 1 TPa, and, also, is smaller than that of BN (870 GPa) and GaN (796 GPa) nanotubes. Kumar et al. (2015) have investigated this parameter for several *zigzag* and *armchair* single-walled AlNNTs, BNNTs and GaNNTs, using the second-generation reactive empirical bond order potential with modified parameters. They showed that for smaller radii of AlNNTs, the Young’s modulus rises with diameter and then reaches a constant value being lower than that of CNTs, BNNTs and GaNNTs.

Poisson’s ratio

Poisson’s ratio ν is another interesting mechanical property that is defined by the nanotube radius variation due to expressing an axial strain on the nanotube:

$$\nu = \frac{\text{Lateral strain}}{\text{Longitudinal strain}} = \frac{\frac{\Delta r}{r_0}}{\frac{\Delta l}{l_0}} , \quad (2)$$

where Δr is the difference between the radius of the strained and that of the unstrained tube, and $\frac{\Delta l}{l_0}$ is the axial strain. The calculated Poisson’s ratio for (3,3) and (5,5) *armchair* AlNNTs is about 0.184 and 0.216 and that for

(9,0), (10,0), and (12,0) zigzag tubes is about 0.269, 0.287, and 0.287, respectively (Kumar et al. 2015). The Poisson's ratio value of zigzag AlNNTs is higher than that of the armchair AlNNTs, indicating that the zigzag AlNNTs are more flexible than the armchair ones.

Shear modulus

Shear modulus or modulus of rigidity is the factor of elasticity regard a shearing force. It is given as the ratio of shear stress to the shear strain. Shear modulus has been theoretically calculated for AlNNTs, GaNNTs and CNTs with different diameters and chiralities (Kumar et al. 2015). The shear modulus of AlNNTs is in the range of 125–175 GPa, which is increased by enlarging the diameter. It is also approximately independent of the tube chirality. The shear modulus of AlNNTs has been predicted to be significantly smaller than that of GaNNTs and CNTs.

Electronic properties

Conductivity

Balasubramanian et al. (2004), using the normalized conductance I–V spectrum, have shown that their synthesized single twisted AlNNTs are metallic in character. This finding is in contrast to the results of theoretical studies which have reported that the AlNNTs are semiconductors (Kang and Hwang 2004; Shi et al. 2005; Ahmadi et al. 2012). Also, the bulk AlN crystal is a large-band-gap semiconductor (Gutiérrez-Sosa et al. 2002). This inconsistency may be due to structural coiling, defects and impurities in the synthesized tubes in comparison to those that are theoretically studied.

HOMO–LUMO gap

The energy difference between the HOMO and LUMO is called the HOMO–LUMO gap which may be used to estimate the strength and kinetic stability of materials, also the colors that they generate in solution, and optical properties (Srivastava et al. 2016; Hesabi and Hesabi 2013; Nagarajan et al. 2014). The change of HOMO–LUMO gap upon a chemical adsorption on a surface has been frequently used as an index of electronic sensitivity (Beheshtian et al. 2012a, b, c, d, e, f, g, h, i, j, 2013a, b, c, d, e; Peyghan et al. 2013a, b, c, 2014). There are no experimental data on this field, while several DFT calculations have predicted the HOMO–LUMO gap for different AlNNTs (Ahmadi et al. 2011a, b, 2012). It should be noted that DFT methods give different values for HOMO, LUMO, and HOMO–LUMO gap, especially, depending on the

percentage of HF exchange of the functional (Zhang and Musgrave 2007). The experimentally obtained AlN band gap is approximately 6.28 eV (Perry and Rutz 1978).

Zhen et al. (2007) have investigated one-dimensional nanostructures of AlN, including faceted nanotubes, nanowires and (12,0) zigzag tubes by means of DFT calculations based on the GGA approach. They revealed that the gap of the AlN nanostructured materials is much narrower than that of the bulk AlN because of the states of surface at the band edges. They predicted that the gap of wurtzite solid AlN is about 4.22 eV and that of (12,0) zigzag single-walled nanotube is about 2.88 eV at the PW91 level of theory. Our DFT results have previously indicated that, the HOMO–LUMO energy gap of AlNNTs enlarged by increasing the diameter of nanotube, in contrast to the semiconducting CNTs (Ahmadi et al. 2011a, b). It has been predicted that the gap is about 3.74, 4.11, 4.17, and 4.27 eV for (4,0), (5,0), (6,0), and (7,0) zigzag AlNNTs, respectively, being larger than the results of Zhen et al. (2007). It is noteworthy to say that GGA methods underestimate the gap, and by increasing HF exchange in the hybrid density functionals, the gap is increased (Xiao et al. 2011; Tran and Blaha 2009; Yang et al. 2004).

Potential applications

Gas adsorption

Different nanotubes have been extensively studied as a gas adsorbent because of their high surface/volume ratios (da Silva 2014; Moradi and Peyghan 2014; Rezaei Sameti and Samadi Jamil 2016; 2012a, b; Rastegar et al. 2015). The AlNNTs include polar Al–N bonds, being suitable for chemical adsorptions, but there are no experimental data in this issue. Several DFT studies have been performed on the many gaseous molecule adsorptions on the exterior surface of AlNNTs with different chiralities by different methods (Mahdavifar and Abbasi 2014; Mahdavifar and Haghbayan 2012; Lim and Lin 2008; Beheshtian et al. 2012a, b, c, d, e, f, g, h, i, j, 2013a, b, c, d, e; Xu et al. 2015; Jiao et al. 2010; Peyghan et al. 2013a, b, c; Samadzadeh et al. 2015; Mahdavifar et al. 2013, 2014). A zigzag AlNNT especially with (5,0) chirality has been used in most of the researches. In Table 1, we have summarized the results of adsorption energies of different gases and ions, method, type of nanotube, and year of publication. Xu et al. (2015) have presented a DFT study on the singlet and triplet O₂ dissociations on the surface of AlNNTs. They demonstrated that the triplet O₂ does not dissociate on AlNNT due to a dissociation barrier higher than 1.48 eV, while singlet O₂ can dissociate with a relatively lower dissociation barrier of 0.74 eV. It has further shown that a

Table 1 Adsorption energy (E_{ads} , kcal/mol) of chemicals on the exterior surface of single-walled AlNNT based on the different DFT methods

| Chemical | Tube | Method/basis set | E_{ads} | Year | References |
|-------------------------------|-------|------------------|------------------|------|---------------------------------|
| H ₂ (dissociation) | (8,0) | PBE/DNP | -2.5 | 2008 | Lim and Lin (2008) |
| NH ₃ | (7,0) | B3LYP/6-31G* | -22.5 | 2011 | Ahmadi et al. (2011b) |
| CO | (6,0) | B3LYP/6-31G* | -5.7 | 2012 | Beheshtian et al. (2012e) |
| O ₂ (triplet) | (8,0) | PW91-D/DNP | -2.5 | 2015 | Xu et al. (2015) |
| SO ₂ | (5,0) | B3LYP/6-31G* | -58.2 | 2012 | Beheshtian et al. (2012f) |
| NO ₂ | (5,0) | B3LYP/6-31G* | -18.4 | 2012 | Beheshtian et al. (2012g) |
| CO ₂ | (6,6) | PW91 | -62.1 | 2010 | Jiao et al. (2010) |
| HCOH | (7,0) | B3LYP/6-31G* | -29.9 | 2012 | Ahmadi et al. (2012) |
| Thiophene | (6,0) | B3LYP/6-31G* | -5.0 | 2013 | Peyghan et al. (2013c) |
| H ₂ S | (5,0) | B3LYP/6-31G* | -11.4 | 2012 | Beheshtian et al. (2012h) |
| F ⁻ | (5,0) | B3LYP/6-31G* | -102.5 | 2015 | Samadzadeh et al. (2015) |
| Cl ⁻ | (5,0) | B3LYP/6-31G* | -1.12 | 2015 | Samadzadeh et al. (2015) |
| Li ⁺ | (5,0) | B3LYP/6-31G* | -3.9 | 2015 | Samadzadeh et al. (2015) |
| Na ⁺ | (5,0) | B3LYP/6-31G* | -2.7 | 2015 | Samadzadeh et al. (2015) |
| HCN | (5,0) | B3LYP/6-31G* | -14.3 | 2013 | Beheshtian et al. (2013d) |
| N ₂ O | (5,0) | B3LYP/6-31G* | -5.7 | 2013 | Beheshtian et al. (2013e) |
| Ethane | (4,4) | PBE | -2.8 | 2014 | MahdaviFar et al. (2014) |
| Ethene | (4,4) | PBE | -6.8 | 2014 | MahdaviFar et al. (2014) |
| Methane | (4,4) | PBE | -2.1 | 2012 | MahdaviFar and Haghbayan (2012) |

high temperature helps the dissociation of singlet O₂ which leads the dissociation barrier to decrease to 0.65 eV at 298.15 K. They studied the dissociation process on the AlNNTs with different chiralities including (8,0) (9,0) (10,0) (11,0) (12,0) (13,0) (14,0) (15,0) and (16,0) zigzag nanotubes. They found that the dissociation barrier reduces with an increase of the nanotube diameter. However, in reality, the O₂ molecule is a triplet with one unpaired electron. Similarly, DFT calculations have shown that NH₃ adsorption energy on the wall of AlNNTs increases with the nanotube diameter reduction (Ahmadi et al. 2011b).

Using DFT calculations, it has been shown that AlNNTs are more reactive than SiC and BN nanotubes to CO₂ molecules (MahdaviFar et al. 2013). The calculated adsorption energies are about -28.0, -3.8, and -2.7 kcal/mol for the adsorption of CO₂ on the wall of SiC, AlN, and BN nanotubes, respectively. Comparative studies on the CO adsorption (Beheshtian et al. 2012a, b, c, d, e, f, g, h, i, j) and H₂ dissociation on the wall of AlN, BN, AlP, and BP nanotubes have been inspected by DFT calculations. The results indicated that among the four studied tubes, the AlNNTs are more appropriate for H₂ dissociation and CO adsorption processes from a kinetic and thermodynamic standpoint. It has been found that the adsorption processes depend on a few factors including the electron density, the nanotube LUMO energy, and length of the linked bonds to the adsorbing atoms and hybridization of the adsorbing atom. Table 1 shows that

most of the gases including ethane, ethene, methane, thiophene, HCN, N₂O, CO, H₂, O₂, H₂S, and NO₂ are physically adsorbed on the surface of AlNNTs with energy releasing below 20.0 kcal/mol.

Chemical sensors

In the recent years, a growing demand in air quality improvement in the living atmosphere has ascended, and it is necessary to screen and standardize chemical exposure in both residential and industrial environments. Thus, great efforts have been dedicated for the development of fast-responding, simple, and highly sensitive devices for chemical detection (Comini et al. 2002; Yamazoe 1991; Yamazoe et al. 1983; Barsan and Weimar 2001). Nanotubes and graphene have attracted strong attention as chemical sensors due to their unique electronic properties and quick response time (Fam et al. 2011; Rastegar et al. 2012; Yoon et al. 2011; Peyghan et al. 2014; Moradi et al. 2013; Peyghan and Moradi 2014a, b). The AlNNTs have been extensively studied as a chemical gas sensor based on DFT calculations. It has been shown that pristine AlNNTs may be a prospective HCOH sensor which can detect this molecule in the presence of water which cannot be sensed by pristine CNTs (Ahmadi et al. 2012). Most of the pristine nanotubes cannot be applied for gas recognition, because the gas does not adsorb on the tube wall due to weak interaction. Thus, extensive computational and

experimental researches have been focused on increasing the performance of sensing properties of nanotubes by structure manipulation (Peng and Cho 2003; Bekyarova et al. 2004; Kar and Choudhury 2013; Zhang et al. 2006; Bai and Zhou 2007; Wang et al. 2007). It is clear that manipulating the structure of adsorbents is very expensive; therefore, it is of great demand to find highly sensitive and perfect nanotubes.

Mahdavifar et al. (2013) have shown that, in comparison to the weak interaction with SiC and BN nanotubes, CO₂ molecule strongly interacts with AlNNT and significantly changes its electrical conductance. They suggested that AlNNT may be employed in nanosensors to recognize the presence of CO₂ molecule. In most of the studies, the sensing mechanism depends on the electrical change based on the below equation (Hadipour et al. 2015):

$$\sigma = A T^{3/2} \exp(-E_g/2kT), \quad (3)$$

where A (electrons/m³K^{3/2}) is a constant, E_g is HOMO–LUMO gap, and k is the Boltzmann's constant. It has been shown that this relation works well for determining the sensitivity of a sensor based on the change of HOMO–LUMO gap (Hadipour et al. 2015). In theoretical studies, the HOMO–LUMO gap is computed after (E_{g2}) and before (E_{g1}) of the adsorption process and the sensitivity is defined as:

$$S = (E_{g2} - E_{g1})/E_{g1} \quad (4)$$

It should be noted that this strategy works for semiconductor adsorbents that their conductivity increases by decreasing the HOMO–LUMO gap.

Single-walled AlNNTs have been presented as an electronic sensor for sensing of SO₂ gas based on DFT calculations (Beheshtian et al. 2012a, b, c, d, e, f, g, h, i, j). The tubes benefit from some advantages which are: high sensitivity: HOMO–LUMO gap of these tubes is remarkably sensitive to the presence of SO₂ gases so that it reduces from 4.11 to 1.01 eV upon the complexation of the tube with the gas; pristine application: these tubes sense the SO₂ gases in its pristine type and the geometry manipulation is not required; short recovery time: interaction energy between the tube and SO₂ gas is not too large to prevent the recovery of sensor; and good selectivity: AlNNTs detect the SO₂ gas in the presence of some other gases such as H₂O, CO, NH₃, N₂, and H₂.

In some cases, it has been shown that the pristine AlNNT cannot detect the chemical, and therefore, a structural manipulation is required (Ahmadi et al. 2012; Beheshtian et al. 2013a, b, c, d, e; Mahdavifar et al. 2014). For example, in contrast to the weak interaction of ethene with the pristine AlNNT, the Ni-decorated AlNNTs exhibit strong affinity toward the ethene molecule with remarkable negative adsorption energies (Mahdavifar et al. 2014). The

electrical conductivity of Ni-decorated AlNNTs is meaningfully sensitive toward ethene and may be employed in the sensor devices (Mahdavifar et al. 2014). In the other study, it was demonstrated that doping an oxygen atom in the vicinity of adsorption site makes the electrical conductivity of AlNNT extremely sensitive to the NH₃ molecule (Ahmadi et al. 2011a, b).

Electron emitters

Favorable optical and field emission properties of nanostructured materials of III–V semiconductors have led to significant interest during the last decade (Padovani and Stratton 1966; Fang et al. 2008; Rideout 1975). Among these, because of the piezoelectric properties, high electrical resistivity and thermal conductivity, the AlN has been used in creating planar display devices and cold cathodes (Taniyasu et al. 2004). AlN has a negative electron affinity, and it has been demonstrated that when some electron emitters are covered by AlN thin films, the field emission is increased (Nemanich et al. 1995). It has been indicated that suitable doping process can fairly increase the AlN field emission properties (Taniyasu et al. 2004). The field emission current is because of the tunneling of electrons from the material into the vacuum through the potential barrier under the impact of an electric field. Thapa et al. (2010) have synthesized AlNNTs filled with Ni nanoparticles, reacting NH₃ gas with Ni–Al thin films. The average diameters of AlNNTs and Ni nanoparticles were 35 and 5 nm, respectively. At room temperature, this structure displayed outstanding field emission, and also a high electrical conductance of approximately about 0.43 k ohm/m. Ni-filled AlNNTs have demonstrated effective field emission with a turn-on field of 15.3 V/mm for an anode–cathode distance of 90 nm (Thapa et al. 2010). The predicted excellent field emission is assumed to be due to the presence of Ni nanoparticle, existence of shallow donor levels and higher surface-to-volume ration of AlNNTs.

Tondare et al. (2002) have reported the field emission measurements from the AlNNTs which were synthesized by the solid–vapor equilibria using gas-phase condensation. The AlNNTs were considered by TEM, and the diameter of the nanotubes was predicted to be in the range of 30–200 nm, and their length from 500 to 700 nm. The AlNNTs have been used in the electron field emitters after the coating on tungsten. Sharp rings were detected in the pattern of the field emission. These rings indicate that the AlNNTs are open-ended. A factor of 34,500 was predicted as the field enhancement, showing that the nanoscale of emitter is a key factor in field emission improvement. Large field enhancement and the observed field emission

patterns of AlNNTs are related to the small nanosize dimensions and properties of polarization. It was predicted that larger diameter nanotubes are more favorable for field emitters because they can be simply tuned (Machado and Azevedo 2011).

Hydrogen storage

Hydrogen, potentially, can be used to provide the energy of mobile industry, but its economical usage has several problems which should be resolved. A difficult challenge is discovery of materials which can store H₂ with a large volumetric and gravimetric density, and work under ambient circumstances. However, hydrogen storage materials should have some standards including minimal gravimetric density (6 wt% by 2010) and optimal adsorption enthalpy per H₂ molecule (0.1–0.2 eV). Wang et al. (2009) have investigated the capability of AlN nanostructures such as AlNNTs to store hydrogen using gradient-corrected DFT. They used the projector augmented wave method (Kresse and Joubert 1999) which was implemented in the Vienna Ab Initio Simulation Package (Kresse and Furthmüller 1996). The structure of Bulk AlN is wurtzite in which the surface of AlNNTs is threefold-, while the Al ions are fourfold-coordinated. Wang et al. (2009) have shown that the unsaturated Al ions with positive charges are favorable adsorption sites for hydrogen gas. They generated a single-walled AlNNT using an (8 × 8 × 2) AlN supercell with wurtzite geometry by eliminating the N and Al atoms from the outer and the inner portion of the two circles along the [0001] path.

After geometry relaxation, the cross-section of AlNNT does not display the structure characteristic of the wurtzite geometry, and the diameter of the nanotube is about 9.463 Å, which is comparable with that of single-walled (9,0) zigzag CNT (Wang et al. 2009). The adsorption energy was predicted to be approximately 0.157 eV/H₂. Calculated bond length between the Al atom of the AlNNT and the hydrogen molecule is about 2.524 Å, and that for H–H bond is 0.753 Å. The hydrogen molecule was predicted to be about 2.620 Å away from the surface of AlNNT. They also investigated the H₂ adsorption in the interior surface of AlNNT. Finally, they reported that the total exterior and interior adsorptions yield a gravimetric density of about 6.15 wt%. It seems that the calculated adsorption energy and gravimetric density are ideal for applications in hydrogen storage industry. Despite these advantages, there are some concerns regarding the possibility of AlNNT applications, and we report some of them in the following: (1) an energy barrier may hinder H₂ molecules from entering the nanotube (Sun et al. 2005). (2) The unsaturated Al atoms in the AlNNTs are very reactive and may attach to unwanted chemicals. (3) The used DFT

method does not correctly present the weak interactions, and dispersion forces are not treated well. (4) The real applications are at room temperatures, but the calculations have been performed at 0 K.

Conclusions

AlNNTs are wide-band-gap nanostructures with high reactivity and electronic sensitivity toward chemicals such as SO₂, NO₂, HCOH, and so on. The experimental band gap is reported to be about 6.28 eV, and computational studies based on the B3LYP method reported a HOMO–LUMO gap in the range of 3.74–4.27 eV for zigzag AlNNTs depending on the diameter. In 2003, the faceted single-crystalline hexagonal AlNNTs were synthesized by nitriding the aluminum powder, and many theoretical works have suggested several potential applications for AlNNTs including chemical sensor, hydrogen storage, gas adsorbent, and electron field emitter. Also, their synthesis has been reported by epitaxial casting and MOCVD growth methods. However, there is still a concern for discovering a method to synthesize a single-walled AlNNT from its AlN sheet similar to the BN or carbon nanotubes. Synthetic research on AlNNTs is in its initial stage, and a few papers related to their synthesis have been published to date. Thus, the present lack of a synthesis method surely limits the applications of AlNNTs. On the other hand, a key feature that has attracted much research effort is the reactivity and electronic sensitivity of AlNNTs. In particular, theoretical studies have shown that AlNNTs can be used in their pristine form as fast, selective and reusable chemical sensors. Compared to CNTs and BNNTs, the research on functionalized AlNNTs with foreign groups has had relatively modest progress and no experimental data have been published on the chemical modifications. The Young's modulus of AlNNTs is about 453 GPa based on the DFT methods and 250–450 based on the experiment.

References

- Ahmadi A, Beheshtian J, Hadipour NL (2011a) Interaction of NH₃ with aluminum nitride nanotube: electrostatic vs. covalent. *Phys E* 43:1717–1719. doi:10.1016/j.physe.2011.05.029
- Ahmadi A, Kamfiroozi M, Beheshtian J, Hadipour NL (2011b) The effect of surface curvature of aluminum nitride nanotubes on the adsorption of NH₃. *Struct Chem* 22(6):1261–1265. doi:10.1007/s11224-011-9820-1
- Ahmadi A, Hadipour NL, Kamfiroozi M, Bagheri Z (2012) Theoretical study of aluminum nitride nanotubes for chemical sensing of formaldehyde. *Sens Actuators B Chem* 161:1025–1029. doi:10.1016/j.snb.2011.12.001
- Almeida EF, de Brito Mota F, de Castilho CMC, Kakanakova-Georgieva A, Gueorguiev GK (2012) Defects in hexagonal-AlN

- sheets by first-principles calculations. *Eur Phys J B* 85(1):1–9. doi:10.1140/epjb/e2011-20538-6
- Altoe MVP, Sprunck JP, Gabriel J-CP, Bradley K (2003) Nanococoon seeds for BN nanotube growth. *J Mater Sci* 38(24):4805–4810. doi:10.1023/b:jmsc.000004399.94881.57
- Baei MT, Peyghan AA, Moghimi M (2012a) Theoretical study of cyano radical adsorption on (6, 0) zigzag single-walled carbon nanotube. *Mon Chem* 143:1–8. doi:10.1007/s00706-012-0739-z
- Baei MT, Peyghan AA, Moghimi M, Hashemian S (2012b) First-principles calculations of structural stability, electronic, and electrical responses of GeC nanotube under electric field effect for use in nanoelectronic devices. *Superlattices Microstruct* 52(6):1119–1130. doi:10.1016/j.spmi.2012.08.011
- Baei MT, Peyghan AA, Bagheri Z (2012c) A computational study of AlN nanotube as an oxygen detector. *Chin Chem Lett* 23:965–968. doi:10.1016/j.cclet.2012.06.027
- Baei MT, Peyghan AA, Bagheri Z (2013) A density functional theory study on acetylene-functionalized BN nanotubes. *Struct Chem* 24(4):1007–1013. doi:10.1007/s11224-012-0129-5
- Bai L, Zhou Z (2007) Computational study of B- or N-doped single-walled carbon nanotubes as NH₃ and NO₂ sensors. *Carbon* 45(10):2105–2110. doi:10.1016/j.carbon.2007.05.019
- Balashubramanian C, Bellucci S, Castrucci P, De Crescenzi M, Boraskar S (2004) Scanning tunneling microscopy observation of coiled aluminum nitride nanotubes. *Chem Phys Lett* 383(1):188–191. doi:10.1016/j.cplett.2003.11.028
- Barsan N, Weimar U (2001) Conduction model of metal oxide gas sensors. *J Electroceram* 7(3):143–167. doi:10.1023/a:1014405811371
- Beheshtian J, Peyghan AA (2013) Theoretical study on the functionalization of BC₂N nanotube with amino groups. *J Mol Model* 19(6):2211–2216. doi:10.1007/s00894-013-1759-2
- Beheshtian J, Peyghan AA, Bagheri Z (2012a) Nitrate adsorption by carbon nanotubes in the vacuum and aqueous phase. *Mon Chem* 143:1623–1626. doi:10.1007/s00706-012-0738-0
- Beheshtian J, Peyghan AA, Bagheri Z (2012b) Quantum chemical study of fluorinated AlN nano-cage. *Appl Surf Sci* 259:631–636. doi:10.1016/j.apsusc.2012.07.088
- Beheshtian J, Peyghan AA, Bagheri Z, Kamfiroozi M (2012c) Interaction of small molecules (NO, H₂, N₂, and CH₄) with BN nanocluster surface. *Struct Chem* 23:1567–1572. doi:10.1007/s11224-012-9970-9
- Beheshtian J, Baei MT, Bagheri Z, Peyghan AA (2012d) Co-adsorption of CO molecules at the open ends of MgO nanotubes. *Struct Chem* 23:1981–1986. doi:10.1007/s11224-012-0021-3
- Beheshtian J, Bagheri Z, Kamfiroozi M, Ahmadi A (2012e) A theoretical study of CO adsorption on aluminum nitride nanotubes. *Struct Chem* 23:653–657. doi:10.1007/s11224-011-9911-z
- Beheshtian J, Baei MT, Peyghan AA, Bagheri Z (2012f) Electronic sensor for sulfide dioxide based on AlN nanotubes: a computational study. *J Mol Model* 18(10):4745–4750. doi:10.1007/s00894-012-1476-2
- Beheshtian J, Baei MT, Bagheri Z, Peyghan AA (2012g) AlN nanotube as a potential electronic sensor for nitrogen dioxide. *Microelectron J* 43(7):452–455. doi:10.1016/j.mejo.2012.04.002
- Beheshtian J, Peyghan AA, Bagheri Z (2012h) A first-principles study of H₂S adsorption and dissociation on the AlN nanotube. *Phys E* 44(9):1963–1968. doi:10.1016/j.physe.2012.06.003
- Beheshtian J, Baei MT, Peyghan AA (2012i) Theoretical study of CO adsorption on the surface of BN, AlN, BP and AIP nanotubes. *Surf Sci* 606(11):981–985
- Beheshtian J, Soleymnabadi H, Kamfiroozi M, Ahmadi A (2012j) The H₂ dissociation on the BN, AlN, BP and AIP nanotubes: a comparative study. *J Mol Model* 18(6):2343–2348. doi:10.1007/s00894-011-1256-4
- Beheshtian J, Tabar MB, Bagheri Z, Peyghan AA (2013a) Exohedral and endohedral adsorption of alkaline earth cations in BN nanocluster. *J Mol Model* 19(3):1445–1450. doi:10.1007/s00894-012-1702-y
- Beheshtian J, Peyghan AA, Bagheri Z (2013b) Formaldehyde adsorption on the interior and exterior surfaces of CN nanotubes. *Struct Chem* 24(4):1331–1337. doi:10.1007/s11224-012-0172-2
- Beheshtian J, Peyghan AA, Noei M (2013c) Sensing behavior of Al and Si doped BC₃ graphenes to formaldehyde. *Sens Actuators B Chem* 181:829–834. doi:10.1016/j.snb.2013.02.086
- Beheshtian J, Peyghan AA, Bagheri Z (2013d) Sensing behavior of Al-rich AlN nanotube toward hydrogen cyanide. *J Mol Model* 19(6):2197–2203. doi:10.1007/s00894-012-1751-2
- Beheshtian J, Baei MT, Peyghan AA, Bagheri Z (2013e) Nitrous oxide adsorption on pristine and Si-doped AlN nanotubes. *J Mol Model* 19(2):943–949. doi:10.1007/s00894-012-1634-6
- Bekyarova E, Davis M, Burch T, Itkis M, Zhao B, Sunshine S, Haddon R (2004) Chemically functionalized single-walled carbon nanotubes as ammonia sensors. *J Phys Chem B* 108(51):19717–19720. doi:10.1021/jp0471857
- Bredas J-L (2014) Mind the gap! *Mater Horiz* 1(1):17–19. doi:10.1039/c3mh00098b
- Choi K, Arita M, Arakawa Y (2012) Selective-area growth of thin GaN nanowires by MOCVD. *J Cryst Growth* 357:58–61. doi:10.1016/j.jcrysgro.2012.07.025
- Comini E, Faglia G, Sberveglieri G, Pan Z, Wang ZL (2002) Stable and highly sensitive gas sensors based on semiconducting oxide nanobelts. *Appl Phys Lett* 81(10):1869–1871. doi:10.1063/1.1504867
- Cui H-J, Shi J-W, Fu M-L (2012) Synthesis and catalytic activity of magnetic cryptomelane-type manganese oxide nanotubes. *J Cluster Sci* 23(3):607–614. doi:10.1007/s10876-012-0478-7
- da Silva LB (2014) Structural and dynamical properties of water confined in carbon nanotubes. *J Nanostruct Chem* 4(2):1–5. doi:10.1007/s40097-014-0104-3
- Fam D, Palaniappan A, Tok A, Liedberg B, Moochhala S (2011) A review on technological aspects influencing commercialization of carbon nanotube sensors. *Sens Actuators B Chem* 157(1):1–7. doi:10.1016/j.snb.2011.03.040
- Fang X, Bando Y, Gautam UK, Ye C, Golberg D (2008) Inorganic semiconductor nanostructures and their field-emission applications. *J Mater Chem* 18:509–522. doi:10.1039/b712874f
- Golberg D, Bando Y, Eremets M, Takemura K, Kurashima K, Yusa H (1996) Nanotubes in boron nitride laser heated at high pressure. *Appl Phys Lett* 69(14):2045–2047. doi:10.1063/1.116874
- Goldberger J, He R, Zhang Y, Lee S, Yan H, Choi H-J, Yang P (2003) Single-crystal gallium nitride nanotubes. *Nature* 422(6932):599–602. doi:10.1038/nature01551
- Goodarzi Z, Maghrebi M, Zavareh AF, Mokhtari-Hosseini Z-B, Ebrahimi-hoseinzadeh B, Zarmi AH, Barshan-tashnizi M (2015) Evaluation of nicotine sensor based on copper nanoparticles and carbon nanotubes. *J Nanostruct Chem* 5(3):237–242. doi:10.1007/s40097-015-0154-1
- Gutiérrez-Sosa A, Bangert U, Harvey A, Fall C, Jones R, Briddon P, Heggie M (2002) Band-gap-related energies of threading dislocations and quantum wells in group-III nitride films as derived from electron energy loss spectroscopy. *Phys Rev B* 66(3):035302. doi:10.1103/physrevb.66.035302
- Hacohen YR, Grunbaum E, Tenne R, Sloan J, Hutchison J (1998) Cage structures and nanotubes of NiCl₂. *Nature* 395:336–337. doi:10.1038/26380
- Hadipour NL, Peyghan AA, Soleymnabadi H (2015) Theoretical study on the Al-doped ZnO nanoclusters for CO chemical sensors. *J Phys Chem C* 119(11):6398–6404. doi:10.1021/jp513019z

- Hesabi M, Hesabi M (2013) The interaction between carbon nanotube and skin anti-cancer drugs: a DFT and NBO approach. *J Nanostruct Chem* 3(1):1–6. doi:10.1186/2193-8865-3-22
- Iijima S (1991) Helical microtubules of graphitic carbon. *Nature* 354:56–58. doi:10.1038/354056a0
- Jiao Y, Du A, Zhu Z, Rudolph V, Smith SC (2010) A density functional theory study of CO₂ and N₂ adsorption on aluminium nitride single walled nanotubes. *J Mater Chem* 20(46):10426–10430. doi:10.1039/c0jm01416h
- Kakanakova-Georgieva A, Persson POÅ, Yakimova R, Hultman L, Janzén E (2004) Sublimation epitaxy of AlN on SiC: growth morphology and structural features. *J Cryst Growth* 273:161–166. doi:10.1016/j.jcrysgro.2004.07.093
- Kakanakova-Georgieva A, Gueorguiev GK, Stafström S, Hultman L, Janzén E (2006) AlGaInN metal-organic-chemical-vapor-deposition gas-phase chemistry in hydrogen and nitrogen diluents: first-principles calculations. *Chem Phys Lett* 431:346–351. doi:10.1016/j.cplett.2006.09.102
- Kang JW, Hwang HJ (2004) Atomistic study of III-nitride nanotubes. *Comput Mater Sci* 31(3):237–246. doi:10.1016/j.commatsci.2004.03.004
- Kar P, Choudhury A (2013) Carboxylic acid functionalized multi-walled carbon nanotube doped polyaniline for chloroform sensors. *Sens Actuators B Chem* 183:25–33. doi:10.1016/j.snb.2013.03.093
- Kim TK, Jeong E, Oh C, Shin M, Kim J, Jung O, Suh H, Khan F, Hyun M, Jin J (2011) Helical silica nanotubes: nanofabrication architecture, transfer of helix and chirality to silica nanotubes. *Chem Pap* 65:863–872. doi:10.2478/s11696-011-0083-5
- Kresse G, Furthmüller J (1996) Efficient iterative schemes for ab initio total-energy calculations using a plane-wave basis set. *Phys Rev B* 54(16):11169–11186. doi:10.1103/physrevb.54.11169
- Kresse G, Joubert D (1999) From ultrasoft pseudopotentials to the projector augmented-wave method. *Phys Rev B* 59(3):1758–1775. doi:10.1103/physrevb.59.1758
- Kumar D, Verma V, Dharamvir K, Bhatti H (2015) Elastic moduli of boron nitride, aluminium nitride and gallium nitride nanotubes using second generation reactive empirical bond order potential. *Multidiscip Model Mater Struct* 11(1):2–15. doi:10.1108/mmms-01-2014-0006
- Lee SM, Lee YH, Hwang YG, Elsner J, Porezag D, Frauenheim T (1999) Stability and electronic structure of GaN nanotubes from density-functional calculations. *Phys Rev B* 60(11):7788–7793. doi:10.1103/physrevb.60.7788
- Lim SH, Lin J (2008) Ab initio study of the hydrogen chemisorption of single-walled aluminum nitride nanotubes. *Chem Phys Lett* 466(4–6):197–204. doi:10.1016/j.cplett.2008.10.059
- Liu Y, Gorla C, Liang S, Emanetoglu N, Lu Y, Shen H, Wraback M (2000) Ultraviolet detectors based on epitaxial ZnO films grown by MOCVD. *J Electron Mater* 29:69–74. doi:10.1007/s11664-000-0097-1
- Machado M, Azevedo S (2011) Stability and electronic properties of AlN nanotubes under the influence of external electric field. *Eur Phys J B* 81(1):121–125. doi:10.1140/epjbe/2011-10687-y
- Mahdavi Z, Abbasi N (2014) The influence of Cu-doping on aluminum nitride, silicon carbide and boron nitride nanotubes' ability to detect carbon dioxide; DFT study. *Phys E* 56:268–276. doi:10.1016/j.physe.2013.09.008
- Mahdavi Z, Haghbayan M (2012) Theoretical investigation of pristine and functionalized AlN and SiC single walled nanotubes as an adsorption candidate for methane. *Appl Surf Sci* 263:553–562. doi:10.1016/j.apsusc.2012.09.106
- Mahdavi Z, Abbasi N, Shakerzadeh E (2013) A comparative theoretical study of CO₂ sensing using inorganic AlN, BN and SiC single walled nanotubes. *Sens Actuators B Chem* 185:512–522. doi:10.1016/j.snb.2013.05.004
- Mahdavi Z, Haghbayan M, Abbasi M (2014) Theoretical investigation of ethane and ethene monitoring using pristine and decorated aluminum nitride and silicon carbide nanotubes. *Sens Actuators B Chem* 196:555–566. doi:10.1016/j.snb.2014.02.048
- Moradi M, Peyghan AA (2014) Role of sodium decoration on the methane storage properties of BC₃ nanosheet. *Struct Chem* 25(4):1083–1090. doi:10.1007/s11224-013-0384-0
- Moradi M, Noei M, Peyghan AA (2013) DFT studies of Si- and Al-doping effects on the acetone sensing properties of BC₃ graphene. *Mol Phys* 111(21):3320–3326. doi:10.1080/00268976.2013.783720
- Nagarajan V, Chandiramouli R, Sriram S, Gopinath P (2014) Quantum chemical studies on the structural and electronic properties of nickel sulphide and iron sulphide nanoclusters. *J Nanostruct Chem* 4(1):1–16. doi:10.1007/s40097-014-0087-0
- Nemanich R, Benjamin M, Bozeman S, Bremser M, King S, Ward B, Davis R, Chen B, Zhang Z, Bernholc J (1995) (Negative) electron affinity of AlN and AlGaIn alloys. *MRS proceedings*. Cambridge University Press, Cambridge, p 777. doi:10.1557/proc-395-777
- Nishizawa J, Kurabayashi T (1983) On the reaction mechanism of GaAs MOCVD. *J Electrochem Soc* 130(2):413–417. doi:10.1149/1.2119722
- Noei M, Ebrahimikia M, Saghapour Y, Khodaverdi M, Salari AA, Ahmaddaghaei N (2015) Removal of ethyl acetylene toxic gas from environmental systems using AlN nanotube. *J Nanostruct Chem* 5(2):213–217. doi:10.1007/s40097-015-0152-3
- Oh D-H, Lee YH (1998) Stability and cap formation mechanism of single-walled carbon nanotubes. *Phys Rev B* 58(11):7407–7412. doi:10.1103/physrevb.58.7407
- Padovani F, Stratton R (1966) Field and thermionic-field emission in Schottky barriers. *Solid State Electron* 9(7):695–707. doi:10.1016/0038-1101(66)90097-9
- Parlayici S, Eskizeybek V, Avcı A, Pehlivan E (2015) Removal of chromium (VI) using activated carbon-supported-functionalized carbon nanotubes. *J Nanostruct Chem* 5(3):255–263. doi:10.1007/s40097-015-0156-z
- Peng S, Cho K (2003) Ab initio study of doped carbon nanotube sensors. *Nano Lett* 3(4):513–517. doi:10.1021/nl034064u
- Pentaleri E, Gubanov V, Boekema C, Fong C (1997) First-principles band-structure calculations of p- and n-type substitutional impurities in zinc-blende aluminum nitride. *Phys Status Solidi (b)* 203(1):149–168. doi:10.1002/1521-3951(199709)203:1<149::aid-pssb149>3.0.co;2-j
- Perry P, Rutz R (1978) The optical absorption edge of single-crystal AlN prepared by a close-spaced vapor process. *Appl Phys Lett* 33(4):319–321. doi:10.1063/1.90354
- Peyghan AA, Bagheri Z (2012) Electronic response of BC₃ nanotube to CS₂ molecules: DFT studies. *Comput Theor Chem* 1008:1–7. doi:10.1016/j.comptc.2012.12.014
- Peyghan AA, Moradi M (2014a) DFT study of ozone dissociation on BC₃ graphene with stone-wales defects. *J Mol Model* 20(1):1–7. doi:10.1007/s00894-014-2071-5
- Peyghan AA, Moradi M (2014b) Influence of antisite defect upon decomposition of nitrous oxide over graphene-analogue SiC. *Thin Solid Films* 552:111–115. doi:10.1016/j.tsf.2013.12.050
- Peyghan AA, Omidvar A, Hadipour NL, Bagheri Z, Kamfiroozi M (2012a) Can aluminum nitride nanotubes detect the toxic NH₃ molecules? *Phys E* 44:1357–1360. doi:10.1016/j.physe.2012.02.018
- Peyghan AA, Baei MT, Hashemian S, Moghimi M (2012b) Adsorption of nitrous oxide on the (6,0) magnesium oxide nanotube. *Chin Chem Lett* 23:1275–1278. doi:10.1016/j.ccllet.2012.09.008

- Peyghan AA, Baei MT, Hashemian S, Torabi P (2013a) Adsorption of CO molecule on AlN nanotubes by parallel electric field. *J Mol Model* 19:859–870. doi:10.1007/s00894-012-1614-x
- Peyghan AA, Noei M, Tabar MB (2013b) A large gap opening of graphene induced by the adsorption of Co on the Al-doped site. *J Mol Model* 19:3007–3014. doi:10.1007/s00894-013-1832-x
- Peyghan AA, Baei MT, Torabi P, Hashemian S (2013c) Adsorption of thiophene on aluminum nitride nanotubes. *Phosphorus Sulfur Silicon Relat Elem* 188(9):1172–1177. doi:10.1080/10426507.2012.737879
- Peyghan AA, Rastegar SF, Hadipour NL (2014) DFT study of NH₃ adsorption on pristine, Ni- and Si-doped graphynes. *Phys Lett A* 378:2184–2190. doi:10.1016/j.physleta.2014.05.016
- Rastegar SF, Peyghan AA, Hadipour NL (2012) Response of Si- and Al-doped graphenes toward HCN: a computational study. *Appl Surf Sci* 265:412–417
- Rastegar SF, Peyghan AA, Soleymnabadi H (2015) Ab initio studies of the interaction of formaldehyde with beryllium oxide nanotube. *Phys E* 68:22–27. doi:10.1016/j.physe.2014.12.005
- Rezaei Sameti M, Samadi Jamil E (2016) The adsorption of CO molecule on pristine, As, B, BAs doped (4,4) armchair AlNNTs: a computational study. *J Nanostruct Chem* 6(3):197–205. doi:10.1007/s40097-015-0183-9
- Rideout V (1975) A review of the theory and technology for ohmic contacts to group III–V compound semiconductors. *Solid State Electron* 18(6):541–550. doi:10.1016/0038-1101(75)90031-3
- Robati D, Bagheriyan S, Rajabi M, Moradi O, Peyghan AA (2016) Effect of electrostatic interaction on the methylene blue and methyl orange adsorption by the pristine and functionalized carbon nanotubes. *Phys E* 83:1–6. doi:10.1016/j.physe.2016.04.005
- Saha M, Das S (2014) Fabrication of a nonenzymatic cholesterol biosensor using carbon nanotubes from coconut oil. *J Nanostruct Chem* 4(1):1–9. doi:10.1007/s40097-014-0094-1
- Samadzadeh M, Rastegar SF, Peyghan AA (2015) F⁻, Cl⁻, Li⁺ and Na⁺ adsorption on AlN nanotube surface: a DFT study. *Phys E* 69:75–80. doi:10.1016/j.physe.2015.01.021
- Santos RB, de Brito Mota F, Rivelino R, Kakanakova-Georgieva A, Gueorguiev GK (2016) Van der Waals stacks of few-layer h-AlN with graphene: an ab initio study of structural, interaction and electronic properties. *Nanotechnology* 27(14):145601. doi:10.1088/0957-4484/27/14/145601
- Shamsudin SM, Mohammad M, Zobir MSA, Asli AN, Bakar AS, Abdullah S, Yahya SSY, Mahmood RM (2013) Synthesis and nucleation-growth mechanism of almost catalyst-free carbon nanotubes grown from Fe-filled sphere-like graphene-shell surface. *J Nanostruct Chem* 3(1):1–12. doi:10.1186/2193-8865-3-13
- Shi S-C, Chen C-F, Chattopadhyay S, Chen K-H, Chen L-C (2005) Field emission from quasi-aligned aluminum nitride nanotips. *Appl Phys Lett* 87(7):073109. doi:10.1063/1.2009838
- Sreekala CSNOA, Indiramma J, Kumar KBSP, Sreelatha KS, Roy MS (2013) Functionalized multi-walled carbon nanotubes for enhanced photocurrent in dye-sensitized solar cells. *J Nanostruct Chem* 3(1):1–8. doi:10.1186/2193-8865-3-19
- Srivastava AK, Pandey SK, Misra N (2016) Structure, energetics, spectral and electronic properties of B₃N₃C₅ heterofullerene. *J Nanostruct Chem* 6(2):103–109. doi:10.1007/s40097-015-0184-8
- Stan G, Ciobanu C, Thayer T, Wang G, Creighton J, Purushotham K, Bendersky L, Cook R (2008) Elastic moduli of faceted aluminum nitride nanotubes measured by contact resonance atomic force microscopy. *Nanotechnology* 20:035706–035711. doi:10.1088/0957-4484/20/3/035706
- Stejskal J, Trchová M, Brožová L, Prokeš J (2009) Reduction of silver nitrate by polyaniline nanotubes to produce silver-polyaniline composites. *Chem Pap* 63:77–83. doi:10.2478/s11696-008-0086-z
- Sun Q, Wang Q, Jena P (2005) Storage of molecular hydrogen in BN cage: energetics and thermal stability. *Nano Lett* 5(7):1273–1277. doi:10.1021/nl050385p
- Taniyasu Y, Kasu M, Makimoto T (2004) Field emission properties of heavily Si-doped AlN in triode-type display structure. *Appl Phys Lett* 84(12):2115–2117. doi:10.1063/1.1689398
- Tenne, Zettl Ak (1996) In: Dresselhaus MS, Dresselhaus G, Avouris P (eds) CNTs: synthesis, structure, properties, and applications. Springer, New York, pp 81–111
- Thapa R, Saha B, Das N, Maiti U, Chattopadhyay K (2010) Self filling of Ni nanoparticles in amorphous AlN nanotubes and its field emission property. *Appl Surf Sci* 256(12):3988–3992. doi:10.1016/j.apsusc.2010.01.062
- Tondare V, Balasubramanian C, Shende S, Joag D, Godbole V, Bhoraskar S, Bhadbhade M (2002) Field emission from open ended aluminum nitride nanotubes. *Appl Phys Lett* 80(25):4813–4815. doi:10.1063/1.1482137
- Tran F, Blaha P (2009) Accurate band gaps of semiconductors and insulators with a semilocal exchange-correlation potential. *Phys Rev Lett* 102(22):226401. doi:10.1103/physrevlett.102.226401
- Wang R, Zhang D, Sun W, Han Z, Liu C (2007) A novel aluminum-doped carbon nanotubes sensor for carbon monoxide. *J Mol Struct (Theochem)* 806(1–3):93–97. doi:10.1016/j.theochem.2006.11.012
- Wang Q, Sun Q, Jena P, Kawazoe Y (2009) Potential of AlN nanostructures as hydrogen storage materials. *ACS Nano* 3(3):621–626. doi:10.1021/nm800815e
- Wu J (2009) When group-III nitrides go infrared: new properties and perspectives. *J Appl Phys* 106(1):011101. doi:10.1063/1.3155798
- Wu Q, Hu Z, Wang X, Lu Y, Chen X, Xu H, Chen Y (2003) Synthesis and characterization of faceted hexagonal aluminum nitride nanotubes. *J Am Chem Soc* 125(34):10176–10177. doi:10.1021/ja0359963
- Xiao H, Tahir-Kheli J, Goddard WA III (2011) Accurate band gaps for semiconductors from density functional theory. *J Phys Chem Lett* 2(3):212–217. doi:10.1021/jz101565j
- Xu X, Ren W, Xu H, Zhang X, Zheng X, Phillips DL, Zhao C (2015) O₂ dissociation on the side wall of aluminum nitride nanotube: a DFT investigation. *Sens Actuators B Chem* 213:139–149. doi:10.1016/j.snb.2015.02.032
- Yamazoe N (1991) New approaches for improving semiconductor gas sensors. *Sens Actuators B Chem* 5(1–4):7–19. doi:10.1016/0925-4005(91)80213-4
- Yamazoe N, Kurokawa Y, Seiyama T (1983) Effects of additives on semiconductor gas sensors. *Sens Actuators* 4:283–289. doi:10.1016/0250-6874(83)85034-3
- Yang S, Olishevski P, Kertesz M (2004) Bandgap calculations for conjugated polymers. *Synth Met* 141(1):171–177. doi:10.1016/j.synthmet.2003.08.019
- Yim W, Stofko E, Zanzucchi P, Pankove J, Ettenberg M, Gilbert S (1973) Epitaxially grown AlN and its optical band gap. *J Appl Phys* 44(1):292–296. doi:10.1063/1.1661876
- Yin LW, Bando Y, Zhu YC, Li MS, Tang C-C, Golberg D (2005) Single-crystalline AlN nanotubes with carbon-layer coatings on the outer and inner surfaces via a multiwalled-carbon-nanotube-template-induced route. *Adv Mater* 17(2):213–217. doi:10.1002/adma.200400105
- Yoon HJ, Yang JH, Zhou Z, Yang SS, Cheng MM-C (2011) Carbon dioxide gas sensor using a graphene sheet. *Sens Actuators B Chem* 157(1):310–313. doi:10.1016/j.snb.2011.03.035
- Zhang G, Musgrave CB (2007) Comparison of DFT methods for molecular orbital eigenvalue calculations. *J Phys Chem A* 111(8):1554–1561. doi:10.1021/jp061633o

- Zhang D, Zhang R (2003) Theoretical prediction on aluminum nitride nanotubes. *Chem Phys Lett* 371(3):426–432. doi:[10.1016/s0009-2614\(03\)00289-6](https://doi.org/10.1016/s0009-2614(03)00289-6)
- Zhang R, Costa J, Bertran E (1996) Role of structural saturation and geometry in the luminescence of silicon-based nanostructured materials. *Phys Rev B* 53(12):7847–7850. doi:[10.1103/physrevb.53.7847](https://doi.org/10.1103/physrevb.53.7847)
- Zhang Y, Zhang Y, Zhang D, Liu C (2006) Novel chemical sensor for cyanides: boron-doped carbon nanotubes. *J Phys Chem B* 110(10):4671–4674. doi:[10.1021/jp0602272](https://doi.org/10.1021/jp0602272)
- Zhao M, Xia Y, Zhang D, Mei L (2003) Stability and electronic structure of AlN nanotubes. *Phys Rev B* 68(23):235415–235420. doi:[10.1103/physrevb.68.235415](https://doi.org/10.1103/physrevb.68.235415)
- Zhen Z, Jijun Z, Yongsheng C, Paul von Ragué S, Zhongfang C (2007) Energetics and electronic structures of AlN nanotubes/wires and their potential application as ammonia sensors. *Nanotechnology* 18(42):424023–424030. doi:[10.1088/0957-4484/18/42/424023](https://doi.org/10.1088/0957-4484/18/42/424023)